

Structural and Electronic Properties of Oxidized Graphene

Jia-An Yan, Lede Xian, and M. Y. Chou

School of Physics, Georgia Institute of Technology, Atlanta, Georgia 30332-0430, USA

(Received 26 March 2009; published 21 August 2009)

We have systematically investigated the effect of oxidation on the structural and electronic properties of graphene based on first-principles calculations. Energetically favorable atomic configurations and building blocks are identified, which contain epoxide and hydroxyl groups in close proximity with each other. Different arrangements of these units yield a local-density approximation band gap over a range of a few eV. These results suggest the possibility of creating and tuning the band gap in graphene by varying the oxidation level and the relative amount of epoxide and hydroxyl functional groups on the surface.

DOI: 10.1103/PhysRevLett.103.086802

PACS numbers: 73.22.-f, 73.61.Wp, 81.07.-b

The prospects of graphene-based nanoelectronics [1,2] have stimulated extensive research activities in recent years. Pristine graphene, with two linear bands crossing at the Dirac point, is a zero-gap material. Therefore, much effort has been devoted to creating an energy gap in graphene-based materials for device applications [3–9]. In particular, an energy gap can be achieved through either nanopatterning [4,6] or chemical functionalization [7–9]. The latter has a greater advantage because of the ease to scale up in the production. A recent experiment has successfully generated a metal-semiconductor-metal junction using epitaxial graphene and a single functionalized graphene sheet (FGS) [7]. Analogous to the combination of Si and SiO₂ in the current generation of microelectronics, the FGS has the potential of being seamlessly integrated with graphene in the fabrication of future nanoelectronics devices. One way to produce FGSs is by exfoliation from graphite oxide (GO), which can have different compositions with various oxidation levels depending on the synthesis processes and conditions. Currently, GO is of particular interest to scientists since chemical reduction of GO has been demonstrated as a promising solution-based route for mass production of graphene [10–15].

The electronic properties of the oxidized layers depend on the detailed chemical structure, which remains unresolved for GO for more than a century with various structural models proposed in the literature [16–20]. Increased conductivity was observed during the reduction of an oxidized graphene sheet prepared from GO [8], but the atomic origin of this behavior is still unknown. A recent high-resolution solid-state ¹³C-NMR measurement [21] has confirmed the existence of C-OH (hydroxyl), C-O-C (epoxide), and *sp*² C units on these layers. The data further indicate that a large fraction of *sp*² C atoms are bonded directly to C atoms in the hydroxyl and epoxide groups, and that a large fraction of C atoms in the hydroxyl and epoxide units are bonded to each other. In order to fully establish the atomic configurations and related electronic properties in this important material, we report results from first-principles calculations that provide a clear picture of

the energetically favorable building blocks and stable phases. Interestingly, various energy gap values are found for structures with different O concentrations, suggesting that the gap is highly tunable by varying the amount of hydroxyl and epoxide on the graphene sheet.

Our theoretical study focuses on the following two key issues: (i) how these functional groups arrange themselves on graphene, and (ii) how these arrangements affect the electronic properties of the graphene sheet. The calculations were carried out using the local-density approximation (LDA) within density-functional theory with a plane wave basis set as implemented in the Vienna *ab initio* simulation package (VASP) [22]. Vanderbilt ultrasoft pseudopotentials [23] are employed. All calculations are done with a plane wave cutoff energy of 500 eV. Results shown in Fig. 1 are obtained using a 5 × 5 graphene unit cell with 5 × 5 × 1 *k*-point sampling. The 5 × 5 unit cell contains 50 C atoms, providing a separation of 12.3 Å for the atomic combinations under investigation. The vertical size of the supercell is 12 Å, so the interaction between the layers is expected to be minimal. The size of the lateral unit cell is individually optimized for different coverages. The optimization of atomic positions proceeds until the change in energy is less than 1 × 10⁻⁶ eV per cell and the force on each atom is less than 0.02 eV/Å.

A single functional group of epoxide or hydroxyl on graphene can induce significant local distortion. With a new bond formed between C and O, the bonding characteristics of the connecting C atoms change from planar *sp*² to distorted *sp*³ hybridization. The structure obtained in our calculation is in good agreement with that reported in previous theoretical studies [24,25]. Of particular interest is the distribution of these functional groups on graphene. A recent atomic force microscope measurement showed that the oxidized graphene sheets appear to have a thickness equal to integer multiples of $h \approx 6.7$ Å [26], indicating that epoxide and hydroxyl are most likely to be present on both sides of the graphene sheet. Hence, all of our calculations have considered possible two-sided configurations.

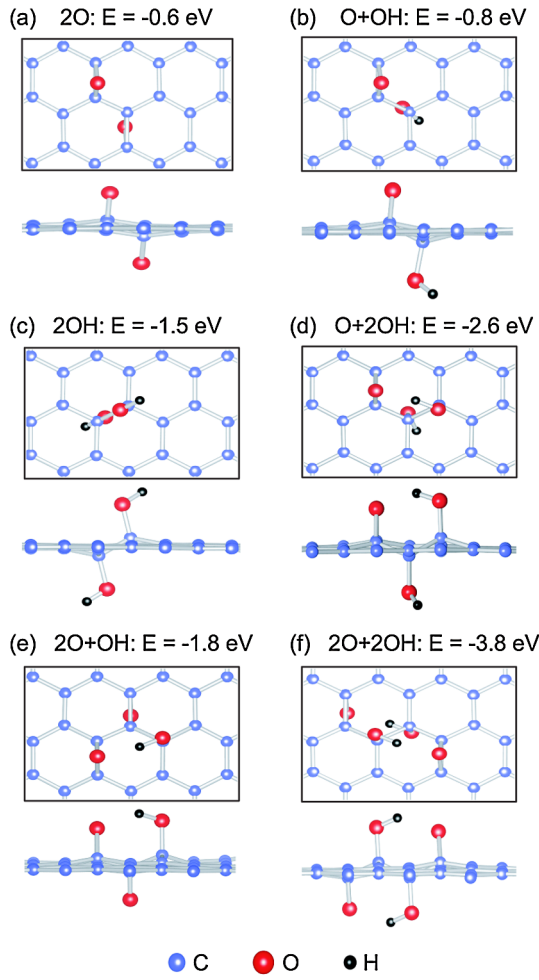


FIG. 1 (color online). Atomic configurations and energies of various favorable combinations of epoxide and hydroxyl groups on the graphene surface. The energy shown is calculated using a 5×5 unit cell and is with respect to the energy sum of well separated individual units on the surface. C and O atoms are represented by large spheres and H by small spheres.

To find out whether these functional groups prefer to aggregate or not, we have calculated the energy change associated with grouping these epoxide and hydroxyl units in various ways, and the results calculated using a 5×5 unit cell are shown in Fig. 1. The energies are referenced to the energy sum of separated individual units on the surface, and the most favorable, fully-relaxed atomic arrangements are shown in Fig. 1 for each combination. As one can see from the figure, the energies are lowered considerably when these epoxide and hydroxyl units are grouped together. Part of the reason is a cancellation of vertical structural distortion when these units can be located on both sides of the sheet. Significant energy gains are found if the OH units form 1,2-hydroxyl pairs [Fig. 1(c)] on opposite sides of the sheet, and the combination of O + 2OH and 2O + 2OH is also especially favorable [Figs. 1(d) and 1(f)]. In Figs. 1(d)–1(f), H points toward the neighboring O on the same side, yielding a configuration characterized by a hydrogen bond. The results in Fig. 1 conclude

that these adsorbed units prefer to aggregate on the graphene surface. This is in full agreement with the experimental results inferred from the NMR data [19–21].

We then explore ordered phases containing epoxide and hydroxyl groups incorporating the energetically favorable building blocks in Fig. 1. Based on the energy results, we only consider arrangements with the OH group appearing in 1,2-hydroxyl pairs. Each periodic phase can be specified by the relative amount of “free” sp^2 C atoms (denoted by C^* , corresponding to C atoms not bonded to O), epoxide (C_2O), and the 1,2-hydroxyl pair [$C_2(OH)_2$ with the connecting C atoms included]. The representative stoichiometry is $C_{1-x-y}^*(C_2O)_x[C_2(OH)_2]_y$, or equivalently $C_{1+x+y}O_x(OH)_{2y}$, with $0 \leq x \leq 1$, $0 \leq y \leq 1$, and $0 \leq x + y \leq 1$. The ordered phases we have calculated are marked on a ternary diagram shown in Fig. 2(a), where the dashed lines indicate phases with the same ratio of epoxide versus the hydroxyl pair. For each phase we investigated, the structure was optimized by exploring various different local arrangements of the epoxide and hydroxyl groups. The lattice parameters and atomic coordinates are fully relaxed. The formation energy is defined in the usual way for a ternary system:

$$\Delta E[x, y] = E[C_{1+x+y}O_x(OH)_{2y}] - (1 - x - y)E[C^*] - xE[C_2O] - yE[C_2(OH)_2], \quad (1)$$

where $E[Z]$ represents the energy of a periodic phase Z . These formation energies are shown in Fig. 2(b) for the

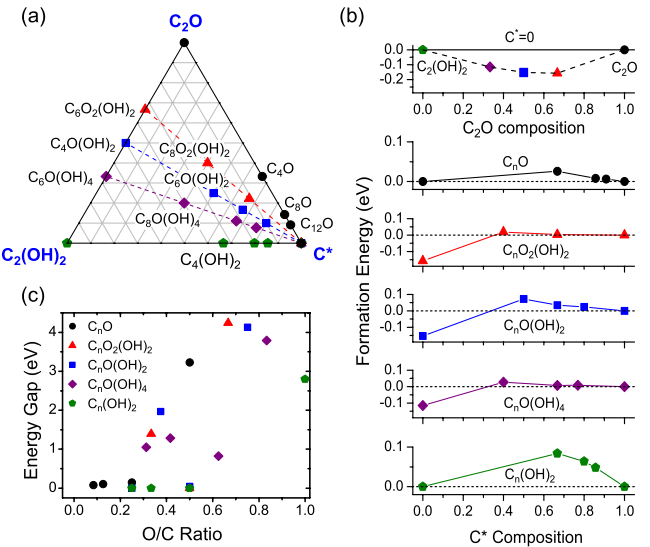


FIG. 2 (color online). (a) Ternary diagram showing ordered phases on the graphene surface with different amounts of sp^2 carbon (C^*), epoxide (C_2O), and the 1,2-hydroxyl pair ($C_2(OH)_2$). The phases investigated in this study are marked on the diagram, with dashed lines indicating those with the same relative amount of epoxide and hydroxyl pairs. (b) Formation energy as defined in Eq. (1) for different phases marked in the ternary diagram in (a). (c) Energy gap as a function of the overall oxygen-to-carbon ratio for different phases.

“binary” phases and for phases along each dashed line in Fig. 2(a).

For the fully-oxidized phases in which all C atoms are bonded to O in either an epoxide or a 1,2-hydroxyl pair, low-energy binary phases with mixed epoxide and hydroxyl compositions are found [top panel of Fig. 2(b)]. These fully-oxidized phases have a lattice expansion of the order of 2%–3%, and an LDA energy gap of 2.8–4.2 eV. With a negative formation energy, these intermediate phases are stable against separation into pure epoxide and pure hydroxyl phases. These stable phases include $C_6O_2(OH)_2$, $C_4O(OH)_2$, and $C_6O(OH)_4$, with an epoxide to hydroxyl ratio of 1:1, 1:2, and 1:4, respectively. As an example, the structure of $C_6O_2(OH)_2$ is shown in Fig. 3(a), in which one can easily identify the following key features: the 1,2-hydroxyl pairs are connected to form a chain-like structure on both sides of the sheet in such a way that the interaction associated with hydrogen bonds can be maximized, and O atoms are drawn to the remaining C atoms in the same hexagonal rings to form epoxides in the close proximity. The other two fully-oxidized phases, $C_4O(OH)_2$, and $C_6O(OH)_4$, follow the same pattern for their atomic arrangements. These features turn out to be quite energetically favorable in constructing phases with intermediate compositions, as will be discussed below. The epoxide-only phase, C_2O , is shown in Fig. 3(b), in which the O atoms follow the arrangements in Fig. 1(a) and stay in rows on opposite sides of the sheet [27]. The buckling is symmetrically compensated. For lower-concentration epoxide-only phases, the opening of the three-membered epoxide ring by breaking the C-C bond to release strain as proposed previously [24] turns out to be energetically favorable, together with the formation of O rows.

Apart from the fully-oxidized “binaries” shown in the top panel of Fig. 2(b), we are not able to find other ordered phases with a negative formation energy. Therefore, the $T = 0$ lowest-energy configuration of the oxidized graphene sheet is likely to be a combination of fully-oxidized regions and the clean graphene phase. This configuration has not been observed experimentally at finite temperature. Possible reasons include the following: the entropy term could be important at finite temperature, the oxidation process is a highly nonequilibrium one, and the covalent bonding in the epoxide and hydroxyl units largely reduces their mobility on the surface. Therefore, domains of various intermediate phases may still be found in the sample under experimental conditions. The relative amount of epoxide and hydroxyl units on the graphene sheet depends on the sample preparation process and can vary over a wide range. Here we focus on phases along each dashed line in Fig. 2(a), in which the relative amount of epoxide and hydroxyl units on the surface is a constant. After exploring various atomic configurations, the lowest-energy periodic structure of these intermediate phases found in our calculation contains strips of epoxide and hydroxyl combinations with clean graphene ribbons in between. An example, the structure of $C_{24}O_2(OH)_8$, is shown in Fig. 3(c), which

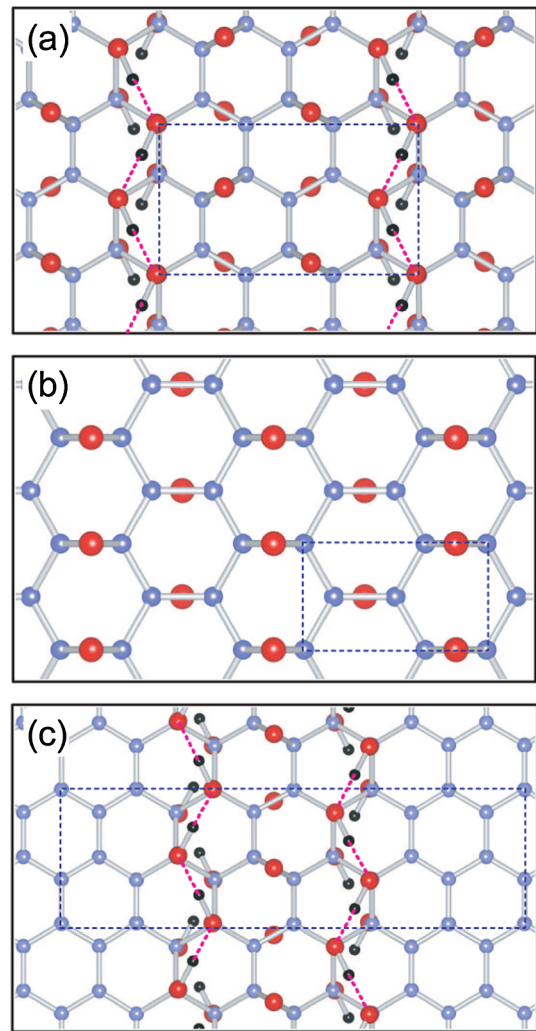


FIG. 3 (color online). Atomic structures for selected phases. (a) Fully-oxidized phase of $C_6O_2(OH)_2$. (b) Fully-oxidized epoxide-only phase C_2O with oxygen rows on both sides of the plane. (c) $C_{24}O_2(OH)_8$ structure with hydroxyl-epoxide strips separated by sp^2 carbon. C and O atoms are represented by large spheres and H by small spheres and the dashed rectangles indicate the respective unit cells. The hydrogen bonds in the hydroxyl chains above the plane are indicated by dashed lines.

contains separate regions of sp^2 and sp^3 carbon. The sp^3 strips consist of double hydroxyl chains and neighboring epoxides. The formation energies for the periodic phases with various intermediate compositions constructed in this fashion are shown in Fig. 2(b). The strips interact weakly when separated by carbon ribbons, which explains why the formation energies of these phases fall on a straight line in Fig. 2(b) when the C^* composition is larger than about 0.4. (Phases with different C^* compositions have different strip separations.) With the formation energies falling on a straight line, many of these phases are expected to coexist on the surface. It is energetically favorable for these strips to coalesce, since the fully-oxidized phase has a lower formation energy. However, this process may not be completed during the oxidation process.

The current results indicate that the configurations investigated in previous density-functional calculations [25] for oxidized graphene sheets containing both the epoxy and hydroxyl groups may not be energetically favorable for a given composition. In our calculation, we find that the formation of hydroxyl chains resulting from hydrogen-bond interaction between neighboring 1,2-hydroxyl pairs greatly lowers the energy and that the epoxides are grouped next to these hydroxyl chains. The epoxide and hydroxyl units randomly deposited on the surfaces are expected to arrange themselves locally following these preferred patterns, giving rise to patches of sp^2 carbon surrounded by fully-oxidized epoxide + hydroxyl regions or vice versa. The possible existence of pure graphene ribbons was proposed previously [28] in order to explain the shift of the Raman peaks in GO and FGSs. The current study provides a strong support for this picture based on extensive first-principles calculations.

The finite region of sp^2 carbon has a consequence in the electronic structure. Without knowing the exact atomic arrangements at various compositions, we use the results of the ordered structures investigated above to provide an estimate for this effect. The calculated LDA energy gaps associated with the ordered phases considered in Fig. 2(a) as a function of the overall O/C ratio are shown in Fig. 2(c). The data-point symbols are the same as those in other parts of Fig. 2. An LDA energy gap of the size ranging from 0 to 4 eV can be found for the range of O concentration we considered. The gap range includes both semiconducting and insulating phases, and the gap size is dictated by the width of the graphene ribbons in the ordered phases we studied. (It is well known that an LDA calculation underestimates the energy gap, and the real gap value is expected to be larger.) A few vanishing band-gap values are associated with armchair ribbons with $3n + 2$ rows of atoms (n is an integer) or zigzag ribbons with an even number of atomic rows. These may be considered as special cases. The overall band-gap results suggest a promising and practical way to tune the energy gap in FGSs by varying the degree of oxidation, which is feasible experimentally, and possibly the location of the oxidized regions.

In summary, with first-principles calculations we have studied the structure and energetics of oxidation functional groups (epoxide and hydroxyl) on single-layer graphene, and the induced changes in the electronic properties. We find that it is energetically favorable for the hydroxyl and epoxide groups to aggregate together and to form specific types of strips with sp^2 carbon regions in between. An LDA band gap ranging from a few tenths of an eV to 4 eV can be obtained by changing the oxidation level and the location of the oxidized region, suggesting a great potential to tune the energy gap in graphene through controlled oxidation processes.

We acknowledge stimulating discussions with W. de Heer, C. Berger, X. Wu, and M. Sprinkle. J. A. Y. thanks D. Pandey for sending a copy of their paper. This work is supported by the Department of Energy (Grant No. DE-FG02-97ER45632). L. X. acknowledges support from the Georgia Tech MRSEC funded by the National Science Foundation (Grant No. DMR-08-20382). This research used computational resources at the National Energy Research Scientific Computing Center, which is supported by the Office of Science of the U.S. Department of Energy under Contract No. DE-AC02-05CH11231, and the National Science Foundation TeraGrid resources provided by the Texas Advanced Computing Center (TACC).

-
- [1] W. A. de Heer *et al.*, Solid State Commun. **143**, 92 (2007).
 - [2] A. K. Geim and K. S. Novoselov, Nature Mater. **6**, 183 (2007).
 - [3] T. Ohta *et al.*, Science **313**, 951 (2006).
 - [4] M. Y. Han *et al.*, Phys. Rev. Lett. **98**, 206805 (2007).
 - [5] G. Giovannetti *et al.*, Phys. Rev. B **76**, 073103 (2007).
 - [6] X. Li *et al.*, Science **319**, 1229 (2008).
 - [7] X. Wu *et al.*, Phys. Rev. Lett. **101**, 026801 (2008).
 - [8] I. Jung *et al.*, Nano Lett. **8**, 4283 (2008).
 - [9] D. C. Elias *et al.*, Science **323**, 610 (2009).
 - [10] H. C. Schniepp *et al.*, J. Phys. Chem. B **110**, 8535 (2006).
 - [11] S. Stankovich *et al.*, Carbon **45**, 1558 (2007).
 - [12] C. Gomez-Navarro *et al.*, Nano Lett. **7**, 3499 (2007).
 - [13] S. Gilje *et al.*, Nano Lett. **7**, 3394 (2007).
 - [14] D. Li *et al.*, Nature Nanotech. **3**, 101 (2008).
 - [15] G. Eda *et al.*, Nature Nanotech. **3**, 270 (2008).
 - [16] T. Nakajima *et al.*, Carbon **26**, 357 (1988).
 - [17] M. Mermoux *et al.*, Carbon **29**, 469 (1991).
 - [18] T. Nakajima and Y. Matsuo, Carbon **32**, 469 (1994).
 - [19] A. Lerf *et al.*, J. Phys. Chem. B **102**, 4477 (1998).
 - [20] H. He *et al.*, Chem. Phys. Lett. **287**, 53 (1998).
 - [21] W. Cai *et al.*, Science **321**, 1815 (2008).
 - [22] G. Kresse and J. Hafner, Phys. Rev. B **47**, 558 (1993).
 - [23] D. Vanderbilt, Phys. Rev. B **41**, 7892 (1990).
 - [24] J.-L. Li *et al.*, Phys. Rev. Lett. **96**, 176101 (2006).
 - [25] D. W. Boukhvalov and M. I. Katsnelson, J. Am. Chem. Soc. **130**, 10697 (2008).
 - [26] D. Pandey *et al.*, Surf. Sci. **602**, 1607 (2008).
 - [27] The fully-oxidized phase C₂O in Fig. 3(b) has a rectangular unit cell of 2.55 Å × 4.40 Å. A recent UHV STM study [26] revealed a local periodicity with a unit cell of 2.73 Å × 4.06 Å in some region of graphene oxide. Despite of a discrepancy of 8%–9% in individual lattice parameters, we note that the area of our calculated unit cell is within 1.2% of the experimental value. We suspect that other causes, for example, the substrate effect, might influence the measured lattice parameters.
 - [28] K. N. Kudin *et al.*, Nano Lett. **8**, 36 (2008).